Transepithelial Projections from Basal Cells Are Luminal Sensors in Pseudostratified Epithelia

Winnie Wai Chi Shum,[1,2] Nicolas Da Silva,[1,2] Mary McKee,[1] Peter J.S. Smith,[3] Dennis Brown,[1,2] and Sylvie Breton[1,2,*]
[1]Center for Systems Biology, Program in Membrane Biology/Nephrology Division, Massachusetts General Hospital, Boston, MA 02114, USA
[2]Harvard Medical School, Boston, MA 02115, USA
[3]BioCurrents Research Center, Molecular Physiology Program, Marine Biological Laboratory, Woods Hole, MA 02543, USA
*Correspondence: sbreton@partners.org
DOI 10.1016/j.cell.2008.10.020

SUMMARY

Basal cells are by definition located on the basolateral side of several epithelia, and they have never been observed reaching the lumen. Using high-resolution 3D confocal imaging, we report that basal cells extend long and slender cytoplasmic projections that not only reach toward the lumen but can cross the tight junction barrier in some epithelia of the male reproductive and respiratory tracts. In this way, the basal cell plasma membrane is exposed to the luminal environment. In the epididymis, in which luminal acidification is crucial for sperm maturation and storage, these projections contain the angiotensin II type 2 receptor (AGTR2). Activation of AGTR2 by luminal angiotensin II, increases proton secretion by adjacent clear cells, which are devoid of AGTR2. We propose a paradigm in which basal cells scan and sense the luminal environment of pseudostratified epithelia and modulate epithelial function by a mechanism involving crosstalk with other epithelial cells.

INTRODUCTION

Epithelial cells have developed complex mechanisms that allow them to detect both apical and basolateral stimuli, and modulate their function in response to physiological demands. The different cell types that comprise specific epithelia must work in a concerted manner to coordinate their barrier function. Previous studies have largely focused on the morphologically dominant epithelial cells in several tissues, whereas basal cells that are nestled beneath these epithelial cells have remained mostly enigmatic. These cells were believed to be restricted to the basal region of pseudostratified epithelia where they may function as stem cells (Ford and Terzaghi-Howe, 1992; Hajj et al., 2007; Ihrler et al., 2002; Lavker et al., 2004; Leung et al., 2007; Rizzo et al., 2005) and participate in basolateral signaling (Evans et al., 2001; Hermo and Robaire, 2002; Ihrler et al., 2002; Leung et al., 2004; van Leenders and Schalken, 2003). We now show that, in contrast to the prevailing view, basal cells of the upper

respiratory tract and the male reproductive tract (epididymis and coagulating gland) extend slender cytoplasmic projections that cross the tight junction (TJ) barrier and reach the epithelial lumen.

The epididymal epithelium, which connects the testis to the vas deferens, forms a tight blood/epididymis barrier and establishes an optimal luminal environment for the maturation and storage of spermatozoa (Hermo and Robaire, 2002; Hinton and Palladino, 1995). Male fertility is partially regulated via the renin-angiotensin system (RAS) located in the tubule lumen (Hagaman et al., 1998; Krege et al., 1995; Leung and Sernia, 2003). Both angiotensin II (ANGII) type 1 and type 2 receptors (AGTR1 and AGTR2) are expressed in the epididymal epithelium (Leung et al., 1997; Leung and Sernia, 2003; Saez et al., 2004). In the kidney collecting duct, which bears a striking functional and cellular resemblance to the epididymal tubule, ANGII increases proton secretion in specialized intercalated cells (Pech et al., 2008; Rothenberger et al., 2007). Similar cells, called clear cells, are also present in the epididymis where they are responsible for luminal acidification (Breton et al., 1996; Brown et al., 1992), which is essential for keeping sperm dormant during maturation and storage (Hinton and Palladino, 1995; Pastor-Soler et al., 2005). In this study, we found that basal cells are the only cells that express AGTR2. These cells contact the lumen of the epithelium where they interact with ANGII. We provide evidence that they then report their findings to neighboring clear cells, which respond by increasing luminal acidification. This process of luminal sampling by so-called basal cells is a novel mechanism for hormonal signaling that might also be generally applicable to other pseudostratified epithelia, including the respiratory tract.

RESULTS

Basal Cells Send Long, Slender Cytoplasmic Projections toward the Lumen

Epididymis sections from rat (16 μm) were labeled for COX1, a marker of basal cells (Leung et al., 2004). While a dense network of basal cells is located at the base of the epithelium confirming previous reports (Clermont and Flannery, 1970; Veri et al., 1993; Yeung et al., 1994), many basal cells exhibit a narrow body extension that infiltrates between other epithelial cells toward the lumen (Figure 1A, arrows). This was confirmed using
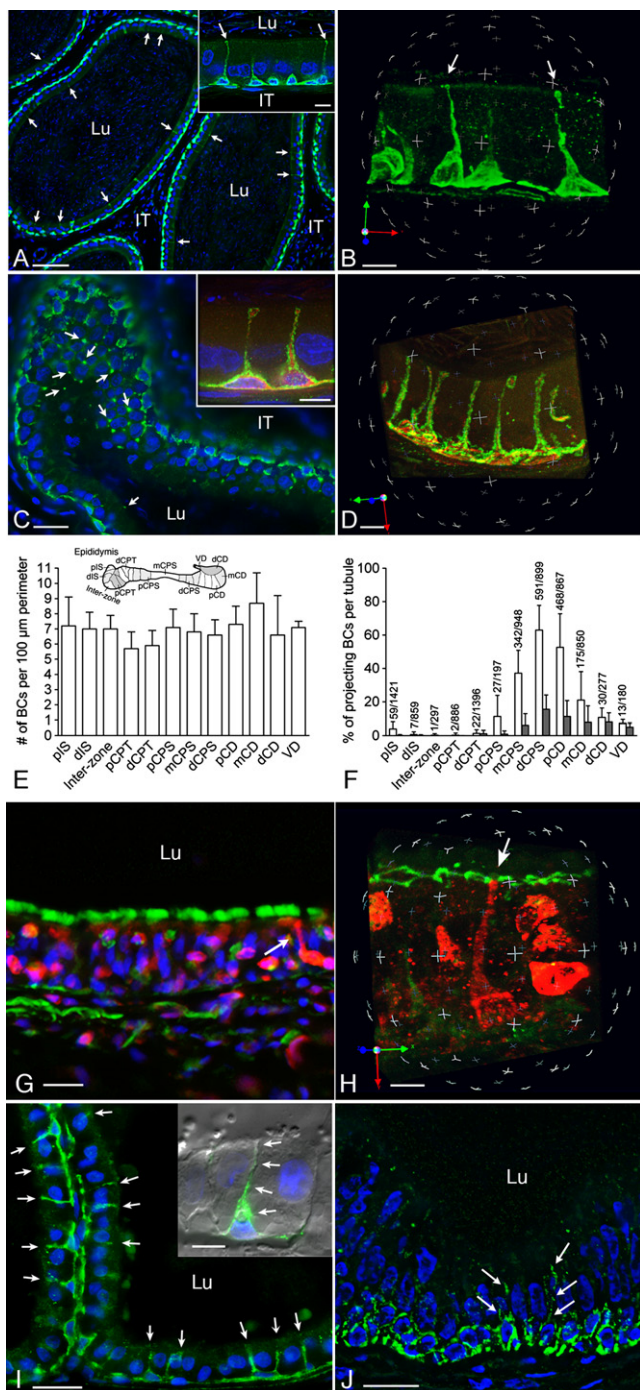
Figure 1. Basal Cells Send Projections toward the Lumen

(A) Rat corpus epididymidis stained for COX1 (green). Higher magnification is shown in inset. Arrows indicate basal cells that extend toward the lumen. The scale bars represent 50 μm and 5 μm (inset).

(B) 3D reconstruction of cauda epididymidis labeled for COX1 (green) showing two basal cells reaching toward the lumen (arrows). See Movie S1. The scale bar represents 8 μm.

(C) Oblique section of cauda epididymidis stained for Cldn1 (green). Basal cell body projections infiltrating between epithelial cells are seen as small dots (arrows). The inset shows two basal cells with intracellular COX1 (red) and membrane-bound Cldn1 (green). The scale bars represent 20 μm and 5 μm (inset).

3D reconstructions from a z-series of confocal images (Figure 1B and Movie S1 available with this article online). The probability of observing these slender structures in thinner sections, which are more commonly used for staining, and in ultrathin sections used for electron microscopy is low, probably explaining why they have not been described extensively in previous publications. Figure 1C shows an oblique section stained for claudin-1 (Cldn1, green), another marker of basal cells (Gregory et al., 2001). Numerous projections, positive for Cldn1, are seen between epithelial cells (arrows). Cldn1 is also present at lower levels in the lateral membrane of principal cells (Gregory et al., 2001), but this was not seen under conditions used in the present study. We did, however, detect basolateral Cldn1 in principal cells using higher concentrations of antibodies (data not shown). The panel C inset shows two basal cells double-stained for COX1 (red) and Cldn1 (green) that extend their narrow body toward the lumen. This result was confirmed by 3D reconstruction (Figure 1D and Movie S2).

A quantitative analysis was performed to determine the number of basal cells reaching the apical pole of the epithelium (defined as the region located above the nuclei of adjacent epithelial cells). Basal cells that projected all the way to the apical border of the epithelium were also counted (Figures 1F). These numbers were normalized for the total number of basal cell nuclei (Figure 1E). Individual epididymis regions and the proximal vas deferens (VD) were analyzed separately. While very few basal cells reached the lumen in the proximal regions, the frequency of events progressively increased toward the distal regions, reaching a maximum in the distal corpus and proximal cauda.

(D) 3D reconstruction of corpus epididymidis double-stained for COX1 (red) and Cldn1 (green) showing several basal cell extensions reaching out to the lumen. See Movie S2. The scale bar represents 8 μm.

(E) Quantification of the total number of basal cells in different regions of the epididymis and the proximal vas deferens. Data are represented as mean ± SEM. No significant differences were detected between the regions. pIS, proximal initial segment; dIS, distal initial segment; Inter-zone, intermediate zone; pCPT, proximal caput; dCPT, distal caput; pCPS, proximal corpus; mCPS, middle corpus; dCPS, distal corpus; pCD, proximal cauda; mCD, middle cauda; dCD, distal cauda; VD, proximal vas deferens.

(F) Open bars: percentage of basal cells detected with their body projection reaching the apical pole of the epithelium. Data are represented as mean ± SEM. Number of cells reaching the apical pole/total number of basal cells are indicated above the bars. Solid bars: percentage of basal cells detected at the apical border.

(G) Rat trachea stained for COX1 (red) and tubulin (green). Arrow shows a COX1-positive basal cell that extends toward the lumen (arrow). The cilia of adjacent ciliated cells are labeled for tubulin. Some unidentified COX1-positive cells are also detected. The scale bar represents 15 μm.

(H) 3D reconstruction of a trachea section double-stained for COX1 (red) and ZO1 (green) showing a basal cell reaching the apical border of the epithelium (arrow). Unidentified COX1-positive cells are also detected. See Movie S3. The scale bar represents 5 μm.

(I) Rat coagulating gland stained for COX1 (green). Several basal cells extend toward the lumen (arrows). The inset shows a COX1-positive basal cell (green) visualized by DIC (arrows). The scale bars represent 15 μm and 5 μm (inset).

(J) Human epididymis 5 μm section stained for COX1 (green). Numerous basal cells are seen in the basal region of the epithelium. Some basal cells are also detected, even on this thinner section, with their body projections reaching the apical region of the epithelium (arrows).
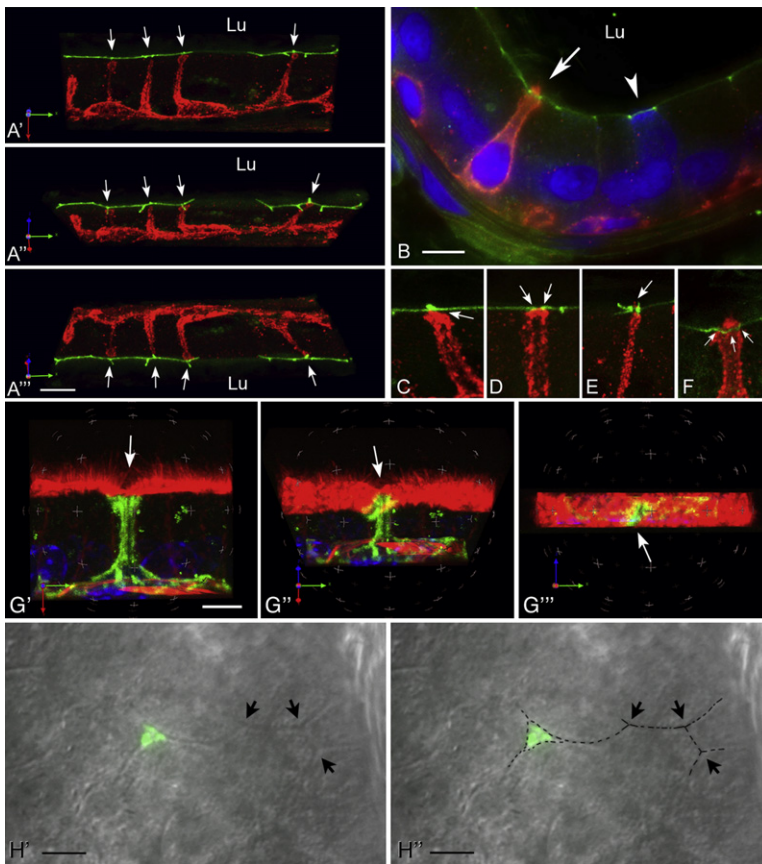
Lu, lumen; IT, interstitium. In some panels, nuclei and spermatozoa are stained in blue with DAPI.

Figure 2. Basal Cells Cross TJs

(A) Three different rotations of a 3D reconstruction of an epididymis section stained for Cldn1 (red) and ZO1 (green). Basal cells reach the TJs at the intersection between three epithelial cells (arrows; see Movie S4). The scale bar represents 10 μm.

(B) Conventional microscopy image of one basal cell (stained for Cldn1 in red) forming a tight junction (stained for ZO1 in green) with adjacent principal cells (arrow). A clear cell expressing apical V-ATPase (blue) is seen (arrowhead). The nuclei are also detected in blue (DAPI). The scale bar represents 5 μm.

(C–F) Body projections of basal cells showing different patterns of interaction with TJs. (C) no colocalization between Cldn1 and ZO1 (arrow; Movie S5); (D) partial colocalization of Cldn1 with ZO1 (arrows; Movie S6); (E) basal cell that penetrates the TJ (arrow; Movie S7); (E) basal cell showing ZO1-stained TJ (green) with adjacent principal cells (arrows; Movie S8).

(G) Rotations of a 3D reconstruction of epididymis stained for Cldn1 (green) and F-actin (red). A Cldn1-positive basal cell reaches the luminal side (arrow) between F-actin-labeled principal cells (see also Movie S9). The scale bar represents 5 μm.

(H) Enface view visualized by DIC and immunofluorescence Cldn1 labeling (green). The dotted lines in H" indicate the junctions between epithelial cells. Arrows show the tricellular corners between epithelial cells. One corner is occupied by a Cldn1-positive basal cell.

In the distal cauda and in the vas deferens, fewer basal cells reached the lumen.

Rat trachea sections (16 μm) were labeled for COX1 (red) and tubulin (green), a marker of airway ciliated cells (Figure 1G). Similarly to the epididymis, some COX1-positive basal cells exhibit a slender projection that extends toward the lumen (arrow). This was confirmed by 3D reconstruction of sections double-stained for ZO1 (green) and COX1 (red) (Figure 1H and Movie S3). While the ZO1-labeled tight junctions (TJs) located at the corner between three epithelial cells (tricellular corners) are closed, the TJ located adjacent to the basal cell apical region is partially open. Basal cells with long cytoplasmic projections in contact with the epithelial apical border were also detected in the larynx (data not shown).

Figure 1I shows that the rat coagulating gland, a tissue morphologically and physiologically analogous to the middle lobe of the human prostate (Price, 1963; Wei et al., 1997), also contains numerous basal cells (stained for COX1 in green; arrows) that send a narrow body projection toward the lumen. The inset is a higher magnification differential interference contrast (DIC) image of a COX1-stained basal cell (green) reaching the luminal border between adjacent epithelial cells (arrows). A dense network of basal cells was also detected in human epididymis stained for Cldn1 (Figure 1J). Importantly, some basal cell extensions were detected even on "thin" 5 μm sections, indicating that these cells have the capacity to reach the lumen in humans also.

Basal Cells Cross TJs to Reach the Lumen

While basal cells were shown to extend processes between epithelial cells, they were never described to have direct access to the lumen (Evans et al., 2001; Hermo and Robaire, 2002; Robaire and Viger, 1995; van Leenders and Schalken, 2003; Veri et al., 1993). To determine whether basal cells can cross the TJ barrier, double labeling for Cldn1 and ZO1 was performed on rat epididymis. Basal cells preferentially reach TJs at the tripartite junction between other epithelial cells (Figure 2A, arrows; Movie S4). Various patterns of interaction between basal cells and TJs were seen. Figure 2B shows a basal cell (arrow) that has crossed the TJ barrier and established contact (labeled with ZO1) with adjacent principal cells. The arrowhead indicates a clear cell with apical V-ATPase labeling (blue). Figures 2C–2F are 3D reconstructions of basal cells showing various patterns of interactions with the TJs. Figure 2C shows one cell underneath the TJ (arrow) but showing no colocalization between Cldn1 and ZO1 (see Movie S5). The yellow staining in Figure 2D (arrows) indicates partial colocalization between the Cldn1-positive basal cell and the ZO1-labeled TJ. The tripartite junction adjacent to this basal cell is partially open (see Movie S6). Figure 2E shows one cell that crosses the TJ barrier (arrow; see also Movie S7). Figure 2F shows one cell that has penetrated the epithelium beyond the TJ barrier and has established contact with adjacent principal cells (arrows and Movie S8; this cell is also shown in Figure 2B). In the trachea, similar patterns of interaction between basal cells and TJs were also seen (see Figure 1H and Movie S3).

The contact of basal cells with the epididymal lumen was further demonstrated with a marker of principal cell apical stereocilia (F-actin). 3D reconstruction clearly showed that basal cells,

stained for Cldn1 (green) but negative for F-actin (arrow), reach the luminal side between principal cells, which are heavily labeled for F-actin (Figure 2G; see also Movie S9). The luminal contact of this basal cell is apparent only on panels showing rotations around the x axis (Figures 2G'' and 2G'''), and is not visible on the XY image shown in Figure 2G'. This is due to the presence of long stereocilia in adjacent principal cells, which mask the small apical pole of the basal cell. The apical surface of a cut-open epididymal tubule was visualized by DIC coupled to Cldn1 labeling (green) (Figure 2H). While most tripartite cell junctions are closed (arrows), one corner is occupied by a Cldn1-positive basal cell, which has established contact with the lumen.

Functional Role of Epididymal Basal Cells

We then examined the potential role of the basal cell extensions. Can these structures scan the lumen for the presence of biological factors? To test this hypothesis, we examined the expression of hormone receptors in these cells. Because luminally located RAS is an important contributor to male fertility, we examined the expression of ANGII receptors in the epididymal epithelium.

Basal Cells Express AGTR2

Double-labeling for the proton-pumping V-ATPase (red), located in the apical pole of clear cells (Figure 3A; arrowheads), and AGTR2 (green) showed that AGTR2 is exclusively expressed in basal cells (arrows). This is in agreement with previous studies showing AGTR2 in the basal region of the epithelium, although the cell type expressing AGTR2 was not identified (Leung et al., 1997). AGTR2 staining was abolished when the antibody was preabsorbed with the immunizing peptide (10-fold excess; Figure 3B). Western blots of rat epididymis showed two bands, one at about 44 kDa, the expected molecular weight of AGTR2, and a second at about 88 kDa (Figure 3C; arrows). Both bands were abolished by preincubation of antibody with its peptide (data not shown). The higher molecular weight band is twice the molecular weight of AGTR2, indicating potential dimerization of AGTR2, as reported for other G protein coupled receptors (Bulenger et al., 2005; Parnot and Kobilka, 2004; Skrabanek et al., 2007). 3D reconstruction (Figure 3D) confirmed that AGTR2 is expressed in basal cells (arrows and Movie S10). Two clear cells stained at their apical pole for the V-ATPase (arrowheads), but negative for AGTR2, are located close to basal cells. The absence of AGTR2 from clear cells was further confirmed by RT-PCR using B1-EGFP transgenic mice in which enhanced GFP is expressed only in clear cells (Miller et al., 2005). Clear cells isolated by fluorescence activated cell sorting (FACS) were compared to GFP-negative cells, i.e., all other cell types in the epididymis. Whereas a positive signal was obtained using primer sets spanning the coding region of *agtr2* in nonclear cells (Figure 3E: GFP-) no signal was detected in clear cells (GFP+). The identity of the PCR product was confirmed by direct sequencing (data not shown).

Basal Cells Sense Luminal ANGII and Regulate Clear Cells via AGTR2

In the kidney, ANGII stimulates proton secretion by intercalated cells (Pech et al., 2008; Rothenberger et al., 2007), which resemble epididymal clear cells (Breton and Brown, 2007). The expression of AGTR2 exclusively in basal cells raised the possibility that
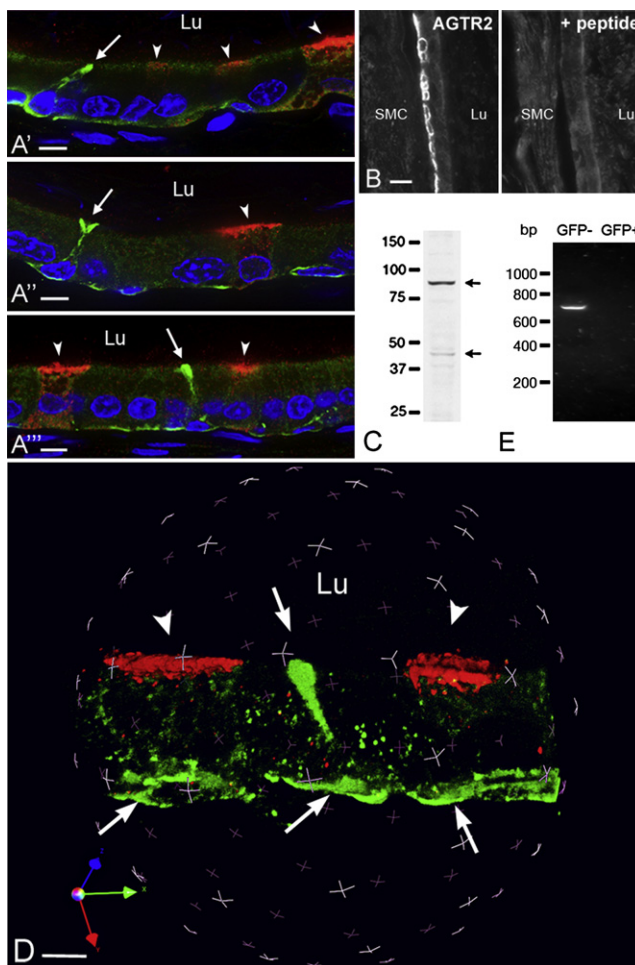

Figure 3. Expression of AGTR2 in Basal Cells

(A) Three examples of AGTR2 (green) and V-ATPase (red) labeling in cauda epididymidis. Arrows indicate AGTR2-labeled basal cells that send projections toward the lumen. Arrowheads show nearby V-ATPase-labeled clear cells. Nuclei are visualized with DAPI (blue). The scale bar represents 5 μm.

(B) Epididymis stained using anti-AGTR2 antibody with (+ peptide) and without (AGTR2) preincubation with the immunizing peptide. The scale bar represents 20 μm.

(C) Western blot detection of AGTR2. 180 μg of epididymal homogenates were loaded onto the gel. Two bands at around 44 and 88 kDa were detected (arrows).

(D) 3D reconstruction showing AGTR2-positive basal cells (green; arrows). One basal cell sends a projection between principal cells. Two clear cells, stained apically for the V-ATPase (red), are visible (arrowheads). See also Movie S10. The scale bar represents 5 μm.

(E) RT-PCR analysis of *Agtr2* mRNA expression in clear cells, isolated by FACS from B1-EGFP mouse epididymides (GFP+), and in all other epididymal cell types (GFP-). While a positive signal was detected in the GFP negative cell population, no *Agtr2* mRNA expression was observed in GFP-positive clear cells.

Lu, lumen; SMC, smooth muscle cells.

these cells might regulate proton secretion by clear cells, following sampling of luminal ANGII. We previously showed that V-ATPase apical membrane accumulation and extension of microvilli in clear cells correlate with proton secretion (Beaulieu
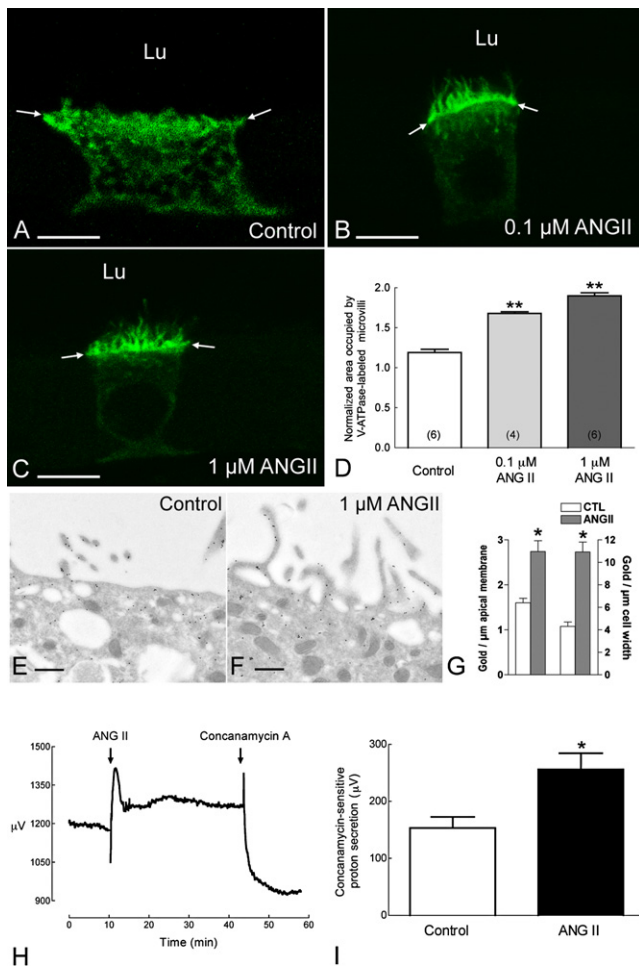
Figure 4. Luminal ANGII Induces V-ATPase Apical Accumulation in Clear Cells

(A–C) Confocal microscopy images of V-ATPase-labeled clear cells (green) luminally perfused in vivo under control conditions (A) or in the presence of 0.1 μM (B) or 1 μM ANGII (C) for 20 min. The arrows show the border between the base of the apical microvilli and the apical pole of the cell. The scale bar represents 5 μm.

(D) Quantitative analysis of the dose-dependent effect of ANGII on the elongation of V-ATPase-labeled microvilli normalized for the apical width of the cell. Values are mean ± SEM obtained from at least 10 cells per epididymis from "n" number of epididymis per group. **$p < 0.001$ versus control.

(E and F) V-ATPase immunogold labeling of the apical pole of a clear cell perfused under control conditions (E) or in the presence of luminal ANGII (1 μM) (F). Under control conditions, the V-ATPase is located mainly in the subapical pole, and a few short V-ATPase-labeled microvilli are detected. In the presence of ANGII, longer and more numerous V-ATPase-labeled microvilli are detected. The scale bar represents 500 nm.

(G) Apical accumulation of V-ATPase by luminal ANGII (1 μM) in clear cells. The left axis shows the density of V-ATPase-associated gold particles in the apical membrane including microvilli (Gold/μm apical membrane). The right axis shows the total number of gold particles located in the apical membrane of clear cells normalized for the width of the cell (Gold/μm cell width). 28 cells were analyzed in each group. Data are expressed as means ± SEM *$p < 0.0005$.

(H) Effect of ANGII (1 μM) on proton secretion in cut-open proximal VD using a proton-selective electrode. After an initial spike due to disturbance of the proton gradient, a sustained increase in proton secretion (expressed as μV)

et al., 2005; Pastor-Soler et al., 2003). Here, we examined the effect of ANGII on the extension of V-ATPase-labeled microvilli.

Rat cauda epididymides were perfused luminally in vivo with phosphate-buffered saline (pH 6.6). Under these control conditions, clear cell V-ATPases are distributed between short microvilli and subapical vesicles (Figure 4A). Addition of ANGII (0.1 and 1 μM) to the luminal perfusate significantly increased the extension of V-ATPase-labeled microvilli to 141 ± 4% and 153 ± 7% versus control, respectively (Figures 4B–4D). Immunogold electron microscopy confirmed this accumulation of V-ATPase in apical microvilli (Figures 4E–4G). ANGII induced a significant increase in the density of V-ATPase molecules in microvilli (G: Gold/μm apical membrane). Because numerous and longer microvilli were observed in clear cells exposed to ANGII, the total number of V-ATPase molecules located at the cell surface was further amplified compared to control (G: Gold/μm cell width).

The effect of ANGII on proton secretion was examined in cut-open proximal VD (Figure 4H), a tissue that also contains clear and basal cells, using an extracellular proton-selective microelectrode (Beaulieu et al., 2005; Breton et al., 1996). After a control period during which stable proton secretion was recorded, ANGII was added to the bath. After a rapid and transient rise due to disturbance of the proton gradient, proton secretion showed a sustained increase. Addition of the V-ATPase inhibitor concanamycin A markedly inhibited proton secretion. For each VD, both the control value (prior to addition of ANGII) and the ANGII value (30 min after its addition) were corrected for the value measured after addition of concanamycin A. On average, ANGII caused a significant increase of concanamycin-sensitive proton secretion of 68% compared to control (Figure 4I). Preincubation of the tissue with concanamycin A for 10 min prevented the response to ANGII (data not shown).

Losartan, an AGTR1 antagonist, had no inhibitory effect on ANGII-induced V-ATPase apical accumulation (Figures 5C and 5D). However the AGTR2 antagonist, PD123319, prevented the stimulatory effect of ANGII on clear cells (Figures 5B and 5D). These results are consistent with participation of AGTR2 in the regulation of clear cell-dependent luminal acidification. Nitric oxide (NO) is the downstream effector of AGTR2 activation (Carey, 2005; Toda et al., 2007). p-cpt-cGMP, a cell-permeable analog of cGMP, or sodium nitroprusside (SNP), a NO-donor, induced a significant elongation of V-ATPase-rich microvilli, compared to control (Figures 6A and 6C). Pretreatment with the soluble guanylate cyclase (sGC) inhibitor ODQ, or the NO synthase (NOS) inhibitor L-NAME, completely abolished ANGII-induced V-ATPase apical accumulation (Figures 6B and 6C). Immunofluorescence labeling showed a strong staining for the $β_1$ subunit of sGC ($β1$-sGC) in the basolateral membrane and apical region of clear cells (Figure 6D: green), identified by apical staining for the V-ATPase (red; arrows). Specificity of the antibody was confirmed by Western blot and immunofluorescence using antibody that had been preabsorbed with $β_1$-sGC peptide (Figures 6E and 6F).

was induced by ANGII. A marked inhibition was then observed following addition of concanamycin A (1 μM).

(I) Mean effect of ANGII (1 μM) on concanamycin-sensitive proton secretion (mean ± SEM, n = 7) measured 30 min after addition of ANGII. *$p < 0.05$.
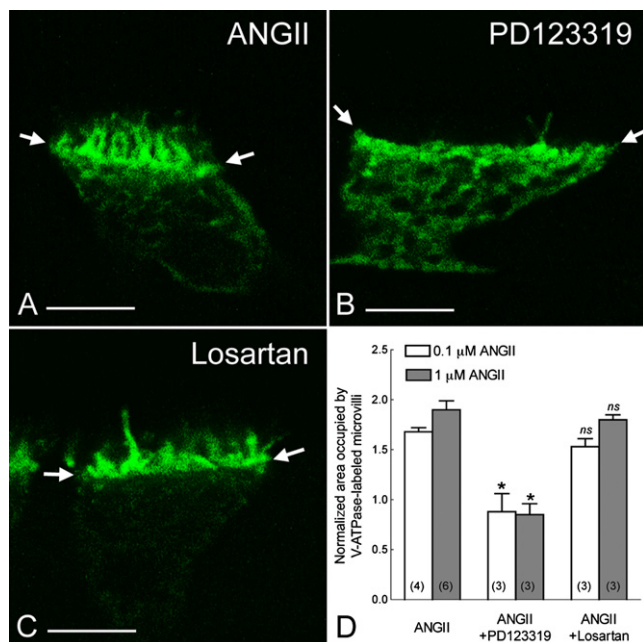
Figure 5. AGTR2 Mediates ANGII-Induced V-ATPase Apical Accumulation and Microvilli Elongation in Clear Cells

(A–C) Confocal images showing clear cells perfused for 20 min with 1 μM ANGII (A), or preincubated for 10 min with PD123319 (1 μM; [B]) or losartan (1 μM; [C]), before addition of ANGII, still in the presence of antagonists. PD123319, but not losartan, prevented the ANGII-induced microvilli elongation. Arrows show the frontier between the base of apical microvilli and the cytoplasm of the cell.

(D) Mean effects of PD123319 and losartan on ANGII-mediated microvilli elongation. PD123319 inhibited the effect of ANGII at both 0.1 and 1 μM concentrations. Values were obtained from at least 10 cells per epididymis. Data are represented as mean ± SEM and "n" is the number of rat epididymis examined. *p < 0.001 versus control; ns: no significant difference versus control.

DISCUSSION

The present study provides evidence that narrow projections emanating from so-called basal cells can actually reach the luminal side of an epithelium. This previously unrecognized property of basal cells was observed in several tissues located in the male reproductive tract and upper respiratory tract, indicating that it is a widespread phenomenon that could have general significance to the biology of pseudostratified epithelia.

In the trachea, two types of basal cells have been described: the so-called basal cells, which appear to nestle beneath columnar epithelial cells, and tall basal cells, which extend processes between other epithelial cells (Evans et al., 2001). Further studies will be required to determine whether these two morphological features are associated with different degrees of body extension in the same population of basal cells, or whether they truly represent two distinct cell populations. Nevertheless, the property of basal cells to reach the luminal border of the epithelium now places these cells in a position to survey foreign pathogenic and allergenic substances that constantly invade the upper respiratory tract.

Two distinct tissues of the male reproductive tract have basal cells that contact the luminal milieu: the coagulating gland and

the epididymis. Interestingly, the coagulating gland in rodents is analogous to the middle lobe of the human prostate (Price, 1963; Wei et al., 1997). The notion that basal cells can reach the prostate lumen will have significant repercussions for our understanding of the (patho)physiology of this important organ. Numerous basal cells reaching toward the lumen were also observed in the rat and human epididymis, indicating that luminal epididymal sampling by basal cells occurs across species.

Basal Cells Cross the TJ Barrier

In the epididymis, we showed that basal cells can cross the blood/epididymis barrier while preserving its integrity. They do so by establishing a new TJ between themselves and adjacent epithelial cells. While sending their body projections toward the lumen, basal cells often seem to "stop short" just beneath the TJs of the epithelium. While virtually no such cells were detected in the proximal regions, the number of basal cells reaching the luminal border dramatically increased in the distal corpus and proximal cauda. This indicates that the capacity of basal cells to reach the lumen is a property that is locally regulated in different regions of the epididymis. A fraction of the total number of basal cells could be seen crossing the TJs at one given time in still images, indicating a potential dynamic interplay between these cells and the epithelium. Thus, basal cells may "come and go" to and from the lumen, and the establishment of a new TJ between basal cells and epithelial cells, in addition to being dynamic, may be temporary. The time required for a leukocyte to cross the TJ barrier of endothelia is less than 2 min (Stein et al., 1997), and it is conceivable that basal cells might modulate the epididymal barrier in a shorter time frame. The signal responsible for inducing basal cells to interact with and cross the TJ barrier remains unclear.

Interestingly, basal cells always reached TJs at the regions where three epithelial cells intersect (tricellular corners), a feature also described for neutrophils crossing endothelial barriers (Burns et al., 2000). Most remarkably, basal cells can actually open up and cross these TJs. The continuous ZO1 labeling in the region of contact between these cells and adjacent epithelial cells suggests that new TJs had been established. High expression of Cldn1 in epididymal basal cells (this study and (Gregory et al., 2001)), as well as in principal cells, at lower levels (Gregory et al., 2001) might provide a molecular "grip" by which basal cells extend projections toward the lumen. Cldn1 forms pairs not only with itself, but also with other claudins, including Cldn3 and Cldn4 (Schneeberger and Lynch, 2004), which are expressed in epididymal TJs (Gregory and Cyr, 2006). This might contribute to the formation of a new TJ between the penetrating basal cell and adjacent epithelial cells. TJ strands constantly form and reform, without disturbing their barrier function (Schneeberger and Lynch, 2004). This remodeling allows migration of leukocytes across endothelia (Burns et al., 2000), as well as penetration of dendritic cells, which also express Cldn1, across the intestinal epithelium (Niess et al., 2005; Rescigno et al., 2001) and the upper respiratory tract (Takano et al., 2005).

Basal Cells Are Luminal Hormone Sensors

The present study also shows that activation of AGTR2 by luminal ANGII stimulates proton secretion by epididymal clear cells
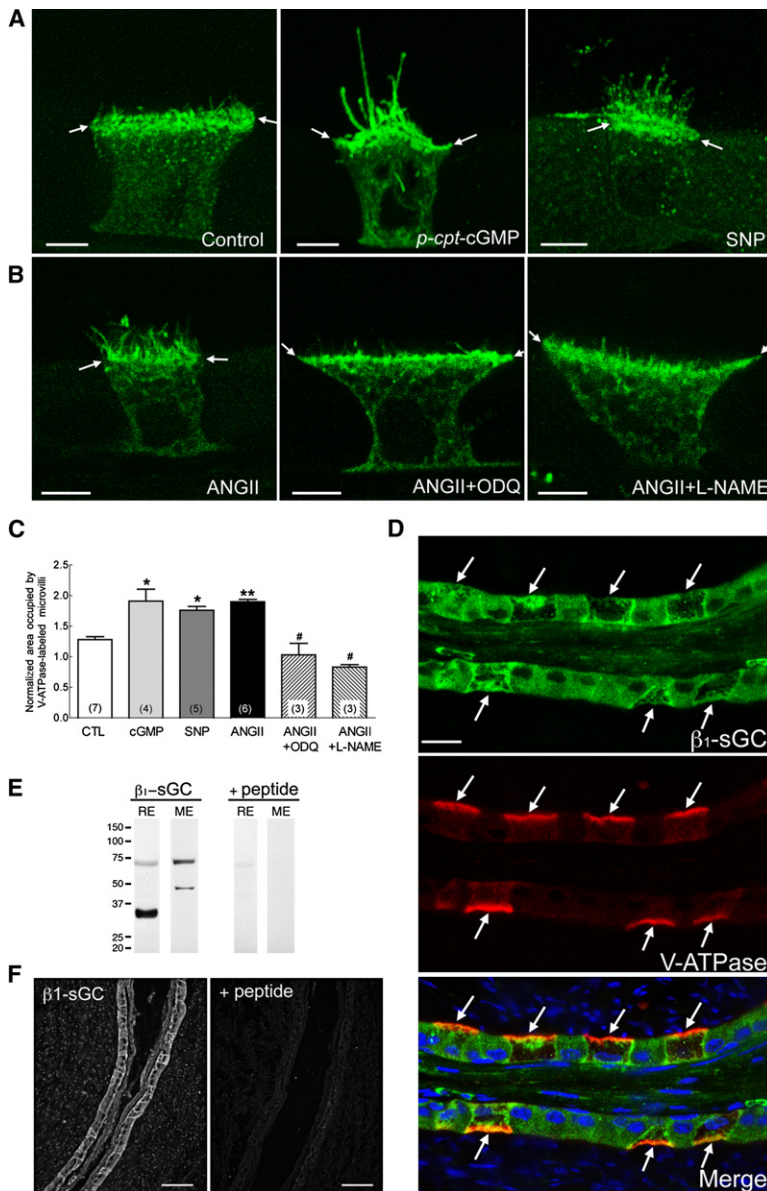
Figure 6. The NO-sGC-cGMP Pathway Mediates ANGII-Induced V-ATPase Apical Accumulation and Microvilli Elongation in Clear Cells

(A) Confocal images of V-ATPase-labeled clear cells (green) perfused under control conditions (control), or in the presence of 1 mM *p-cpt*-cGMP, or 1 mM SNP for 20 min. A marked elongation of V-ATPase-labeled microvilli is observed in the presence of *p-cpt*-cGMP and SNP, compared to control. The arrows indicate the border between the base of apical microvilli and the cytoplasm. The scale bars represent 5 μm.

(B) Effect of ODQ or L-NAME on the ANGII-induced response. Pretreatment for 10 min with ODQ (3 μM) or L-NAME (100 μM), followed by ANGII still in the presence of inhibitors for 20 min, abolished the V-ATPase apical accumulation and microvilli elongation induced by ANGII alone. The scales bar represent 5 μm.

(C) Mean microvilli elongation in clear cells. Values were obtained from at least 10 cells per epididymis. Data are represented as mean ± SEM, and "n" is the number of epididymides examined. *$p < 0.01$ versus control (CTL), **$p < 0.001$ versus CTL, and #$p < 0.001$ versus ANGII.

(D) Localization of β_1-sGC (green) and V-ATPase (red) in epididymis. V-ATPase-positive clear cells (arrows) show abundant β_1-sGC staining in their basolateral membrane and apical pole. Weaker and more uniform staining is also detected in principal, basal, and smooth muscle cells. Nuclei are visualized with DAPI (blue) in the merged panel. The scale bar represents 10 μm.

(E) Western blot detection of β_1-sGC in rat (RE) and mouse epididymis (ME) (120 μg/lane). In both samples, a band at about 70 kDa was detected corresponding to the molecular weight of β_1-sGC. Additional bands at around 35 kDa and 50 kDa were also detected in rat and mouse epididymis, respectively, possibly indicating degradation products in these tissues. All bands were absent after preincubation of the antibody with the immunizing peptide.

(F) Inhibition of immunofluorescence staining using the antibody preincubated with the immunizing peptide (+ peptide). The scale bars represent 50 μm.

via activation of the NO/cGMP pathway. NO is a downstream effector of AGTR2 and because basal cells are the only cell type in which this receptor is expressed, they are the likely site for ANGII-induced NO production. However, determination of the exact cellular origin of NO following AGTR2 activation will require novel tools and animal models for the measurement of NO in single basal cells. A schematic view of our current cell-cell crosstalk model for activation of proton secretion in clear cells following AGTR2 stimulation in basal cells is illustrated in Figure 7. Consistent with this model, endothelial NO synthases (eNOS) have been detected in basal-like cells in human and bovine epididymis (Mewe et al., 2006; Zini et al., 1996). Sampling of luminal ANGII by basal cells followed by activation of proton secretion by clear cells would ensure that the luminal fluid is maintained at its physiological acidic pH. Crosstalk between basal and principal cells has also been proposed to modulate anion secretion by principal cells in response to basolateral lysylbradykinin (Cheung et al., 2005; Leung et al., 2004).

Basolateral stimulation of AGTR1 by ANGII activates anion secretion in cultured principal cells (Leung et al., 1997; Leung and Sernia, 2003), and we now show that the epididymis can respond to luminal ANGII. In agreement with our study, recent reports showed that ANGII increases V-ATPase-dependent proton extrusion by renal intercalated cells (Pech et al., 2008; Rothenberger et al., 2007), which are analogous to clear cells (Breton and Brown, 2007). We have previously shown that cAMP elevation following activation of the bicarbonate sensitive soluble adenylyl cyclase (sAC) and PKA, induced apical accumulation of the V-ATPase into well-developed microvilli in clear cells (Pastor-Soler et al., 2003, 2008). The present study shows that cGMP can also activate V-ATPase-dependent luminal acidification; the mechanism by which this occurs is the subject of ongoing work.

Spermatozoa require an acidic environment to prevent their premature activation during maturation and storage in the epididymis (Hinton and Palladino, 1995; Jones and Murdoch,
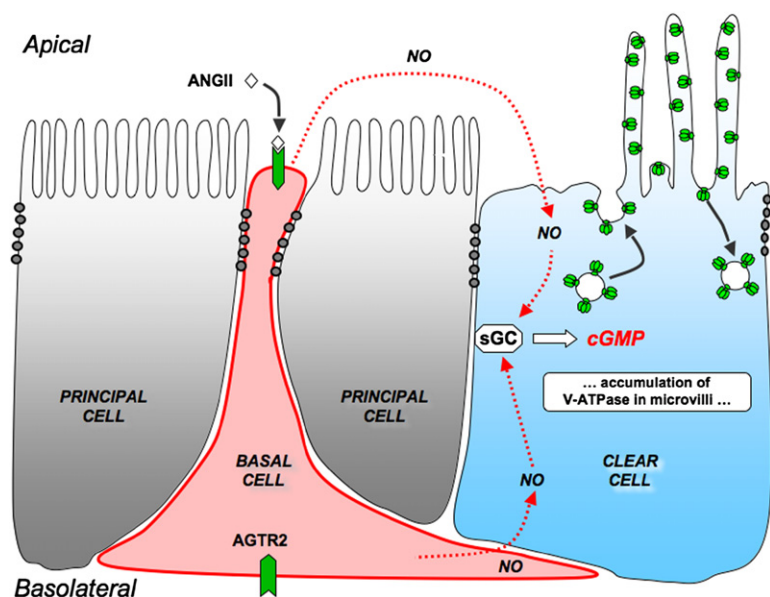
Figure 7. Schematic Representation of Cell-to-Cell Crosstalk in the Epididymal Epithelium

Basal cells extend narrow projections between epithelial cells to reach the lumen. A new TJ is formed between the basal cell and adjacent epithelial cells. Basal cells express AGTR2 and luminal ANGII triggers the production of NO in these cells. NO then acts locally on clear cells to produce cGMP via activation of the sGC, which is enriched in these cells. cGMP induces the accumulation of V-ATPase in well developed apical microvilli in clear cells, which results in the increase of proton secretion.

1996; Pastor-Soler et al., 2005). However, the mechanisms by which spermatozoa interact with epithelial cells of the epididymal tubule remain, for the most part, unknown. In ACE KO mice, absence of the germinal form of ACE (gACE) induces a marked reduction in the quality of sperm, which are unable to fertilize an egg (Esther et al., 1996; Hagaman et al., 1998; Krege et al., 1995). gACE, which is linked to the sperm membrane (Kondoh et al., 2005), is shed from the sperm surface as they mature in the epididymis (Gatti et al., 1999), providing a potential means by which spermatozoa communicate with surrounding epithelial cells. The lack of luminal ANGII in ACE KO male mice might impair the acidifying capacity of the epididymis with detrimental consequences on sperm quality. Indeed, FOXI-1 KO male mice, which have impaired luminal acidification, are also infertile due to sperm inability to fertilize an egg (Blomqvist et al., 2006). Thus, the concerted interaction between sperm, basal cells and clear cells might represent a complex process by which the epididymal epithelium establishes and modulates the appropriate luminal environment for the maturation and storage of sperm.

While we have focused on the regulation of luminal acidification in the male reproductive tract, we propose that sensing and signaling by transepithelial basal cells represents a novel mechanism of cellular crosstalk and functional regulation in pseudostratified epithelia.

SUMMARY

Here, we show that basal cells project slender body extensions that reach the luminal border of pseudostratified epithelia. In the male reproductive tract, basal cells cross the blood/epididymis barrier to monitor luminal factors. We also provide evidence for the presence of a novel crosstalk between basal cells and clear cells to control V-ATPase-dependent proton secretion, a process that is crucial for maintaining sperm quiescent during their maturation and storage in the epididymis. Luminal sampling by basal cells has not been recognized previously and will pro-

vide a new framework for future studies aimed at unraveling the cellular mechanisms by which epithelia respond to luminal stimuli.

EXPERIMENTAL PROCEDURES

Tissue Fixation and Preparation

Adult male Sprague Dawley rats (Charles River Labs, Wilmington, MA) were anesthetized with nembutal (60 mg/kg, i.p.). The male reproductive and upper respiratory tracts were fixed by perfusion through the left ventricle with paraformaldehyde-lysine-periodate (PLP) fixative, as described previously (Pastor-Soler et al., 2003). All procedures were approved by the Massachusetts General Hospital Institutional Committee on Research Animal Use.

In Vivo Microperfusion

Rats were anesthetized and the cauda epididymidis was luminally perfused in vivo, harvested and fixed in PLP, as described previously (Beaulieu et al., 2005; Pastor-Soler et al., 2003; Wong and Yeung, 1978).

Immunofluorescence

Immunofluorescence labeling was performed on cryostat sections, as described previously (Beaulieu et al., 2005; Pastor-Soler et al., 2003). Primary antibodies, the AGTR2 peptide and secondary antibodies used are listed in supplementary material. Slides were mounted in Vectashield (Vector Labs, Burlingame, CA) with or without DAPI. For confocal microscopy, nuclei were stained using TOPRO-3 iodide (Invitrogen, Carlsbad, CA). Immunostained sections were examined using a Nikon E800 microscope (Nikon Instruments, Melville, NY). Digital images were acquired with IPLab Spectrum software (Scanalytics, Fairfax, VA) and imported into Adobe Photoshop. Sections were also examined using a Zeiss Radiance 2000 confocal microscope (Zeiss Laboratories). Z-series (0.1 μm interval) were imported into Volocity software (Improvision Inc., version 4.1) for 3D reconstruction and final animations were exported as Quicktime movies.

Quantification of V-ATPase Apical Membrane Accumulation in Clear Cells

The level of accumulation of V-ATPase in clear cell microvilli was quantified using IPLab software as described previously (Beaulieu et al., 2005; Pastor-Soler et al., 2003). 10 μm sections of microperfused cauda epididymidis were immunostained under identical conditions, and confocal images were acquired using the same parameters. The segmentation procedure of IPLab was used to measure the area of V-ATPase-positive microvilli, which was normalized against the length of apical pole of each cell (Beaulieu et al., 2005; Pastor-Soler et al., 2003). At least three epididymides from different animals were perfused for each condition, and a minimum of 10 cells/tissue were examined for a total of at least 30 cells/condition.

Immunogold Electron Microscopy and Quantification of Gold Labeling

Pieces of PLP-fixed epididymis were embedded at −45°C using HM20 resin (Electron Microscopy Sciences, Hatfield, PA) in a Leica EM AFS, and ultrathin

sections were cut, as described previously (Da Silva et al., 2007; Pastor-Soler et al., 2003). Sections were immunostained for the V-ATPase A subunit, followed by goat anti-rabbit IgG coupled to 15 nm gold (Ted Pella, Reading, CA). Grids were examined in a JEOL 1011 electron microscope. Images were acquired using an AMT digital imaging system.

The number of V-ATPase associated gold particles on the apical membrane and microvilli was counted for each clear cell (Da Silva et al., 2007; Pastor-Soler et al., 2003). To determine the density of V-ATPase molecules along the apical membrane, the number of gold particles was divided by the length of apical membrane, including microvilli, of each cell. This value is referred to as "gold/μm apical membrane." To determine the relative density of the V-ATPase at the cell surface, the number of gold particles was normalized for the width of the cell, measured at the base of the microvilli (gold/μm cell width).

Western Blotting
Protein extracts from rat and mouse epididymis were subjected to electrophoresis and western blotting, as described previously (Beaulieu et al., 2005; Pastor-Soler et al., 2003).

Isolation of Clear Cells, RNA Extraction, and RT-PCR
Epididymides from B1-EGFP transgenic mice (Miller et al., 2005) were digested with trypsin and collagenase. Fluorescence-activated cell sorting (FACS) was used to separate clear cells (GFP-positive) from other cell types (GFP-negative). Total RNA was isolated using the PicoPure RNA Isolation kit (Molecular Devices, Sunnyvale, CA), and RT-PCR was performed as described previously (Isnard-Bagnis et al., 2003). The primers amplifying a 674 bp fragment of the mouse *Agtr2* coding sequence are: attggcttttggacctgtg (MAGTR2-F3) and aaacacactgcggagcttct (MAGTR2-R2). The PCR product was purified with the Qiaquick PCR kit and sequenced by the MGH sequencing core.

Detection of Proton Secretion
The proximal VD was cut open to expose the apical surface of the epithelium and anchored onto a custom-made chamber. Proton secretion was measured using a self-referencing proton-selective electrode, as described previously (Beaulieu et al., 2005; Breton et al., 1996; Smith et al., 2007).

Statistical Analysis
The effects of treatments between two groups were determined by paired or unpaired Student's t test when appropriate. Comparisons between multigroups were determined by one-way ANOVA with Bonferroni's post hoc test. All tests were two-tailed and the limit of statistical significance was set at p = 0.05.

SUPPLEMENTAL DATA

Supplemental Data include Supplemental Experimental Procedures and ten movies and can be found with this article online at http://www.cell.com/supplemental/S0092-8674(08)01312-3.

REFERENCES

Beaulieu, V., Da Silva, N., Pastor-Soler, N., Brown, C.R., Smith, P.J., Brown, D., and Breton, S. (2005). Modulation of the actin cytoskeleton via gelsolin regulates vacuolar H+-ATPase recycling. J. Biol. Chem. *280*, 8452–8463.

Blomqvist, S.R., Vidarsson, H., Soder, O., and Enerback, S. (2006). Epididymal expression of the forkhead transcription factor Foxi1 is required for male fertility. EMBO J. *25*, 4131–4141.

Breton, S., and Brown, D. (2007). New insights into the regulation of V-ATPase-dependent proton secretion. Am. J. Physiol. Renal Physiol. *292*, F1–F10.

Breton, S., Smith, P.J., Lui, B., and Brown, D. (1996). Acidification of the male reproductive tract by a proton pumping (H+)-ATPase. Nat. Med. *2*, 470–472.

Brown, D., Lui, B., Gluck, S., and Sabolic, I. (1992). A plasma membrane proton ATPase in specialized cells of rat epididymis. Am. J. Physiol. *263*, C913–C916.

Bulenger, S., Marullo, S., and Bouvier, M. (2005). Emerging role of homo- and heterodimerization in G-protein-coupled receptor biosynthesis and maturation. Trends Pharmacol. Sci. *26*, 131–137.

Burns, A.R., Bowden, R.A., MacDonell, S.D., Walker, D.C., Odebunmi, T.O., Donnachie, E.M., Simon, S.I., Entman, M.L., and Smith, C.W. (2000). Analysis of tight junctions during neutrophil transendothelial migration. J. Cell Sci. *113*, 45–57.

Carey, R.M. (2005). Update on the role of the AT2 receptor. Curr. Opin. Nephrol. Hypertens. *14*, 67–71.

Cheung, K.H., Leung, G.P., Leung, M.C., Shum, W.W., Zhou, W.L., and Wong, P.Y. (2005). Cell-cell interaction underlies formation of fluid in the male reproductive tract of the rat. J. Gen. Physiol. *125*, 443–454.

Clermont, Y., and Flannery, J. (1970). Mitotic activity in the epithelium of the epididymis in young and old adult rats. Biol. Reprod. *3*, 283–292.

Da Silva, N., Shum, W.W., El-Annan, J., Paunescu, T.G., McKee, M., Smith, P.J., Brown, D., and Breton, S. (2007). Relocalization of the V-ATPase B2 subunit to the apical membrane of epididymal clear cells of mice deficient in the B1 subunit. Am. J. Physiol. Cell Physiol. *293*, C199–C210.

Esther, C.R., Jr., Howard, T.E., Marino, E.M., Goddard, J.M., Capecchi, M.R., and Bernstein, K.E. (1996). Mice lacking angiotensin-converting enzyme have low blood pressure, renal pathology, and reduced male fertility. Lab. Invest. *74*, 953–965.

Evans, M.J., Van Winkle, L.S., Fanucchi, M.V., and Plopper, C.G. (2001). Cellular and molecular characteristics of basal cells in airway epithelium. Exp. Lung Res. *27*, 401–415.

Ford, J.R., and Terzaghi-Howe, M. (1992). Basal cells are the progenitors of primary tracheal epithelial cell cultures. Exp. Cell Res. *198*, 69–77.

Gatti, J.L., Druart, X., Guerin, Y., Dacheux, F., and Dacheux, J.L. (1999). A 105- to 94-kilodalton protein in the epididymal fluids of domestic mammals is angiotensin I-converting enzyme (ACE); evidence that sperm are the source of this ACE. Biol. Reprod. *60*, 937–945.

Gregory, M., and Cyr, D.G. (2006). Identification of multiple claudins in the rat epididymis. Mol. Reprod. Dev. *73*, 580–588.

Gregory, M., Dufresne, J., Hermo, L., and Cyr, D. (2001). Claudin-1 is not restricted to tight junctions in the rat epididymis. Endocrinology *142*, 854–863.

Hagaman, J.R., Moyer, J.S., Bachman, E.S., Sibony, M., Magyar, P.L., Welch, J.E., Smithies, O., Krege, J.H., and O'Brien, D.A. (1998). Angiotensin-converting enzyme and male fertility. Proc. Natl. Acad. Sci. USA *95*, 2552–2557.

Hajj, R., Baranek, T., Le Naour, R., Lesimple, P., Puchelle, E., and Coraux, C. (2007). Basal cells of the human adult airway surface epithelium retain transit-amplifying cell properties. Stem Cells *25*, 139–148.

Hermo, L., and Robaire, B. (2002). Epididymal cell types and their functions. In The Epididymis: From Molecules to Clinical Practice, B. Robaire and B.T. Hinton, eds. (New York: Kluwer Acedemic/Plenum Publishers), pp. 81–102.

Hinton, B.T., and Palladino, M.A. (1995). Epididymal epithelium: its contribution to the formation of a luminal fluid microenvironment. Microsc. Res. Tech. *30*, 67–81.

Ihrler, S., Zietz, C., Sendelhofert, A., Lang, S., Blasenbreu-Vogt, S., and Lohrs, U. (2002). A morphogenetic concept of salivary duct regeneration and metaplasia. Virchows Arch. *440*, 519–526.

Isnard-Bagnis, C., Da Silva, N., Beaulieu, V., Yu, A.S., Brown, D., and Breton, S. (2003). Detection of ClC-3 and ClC-5 in epididymal epithelium:

immunofluorescence and RT-PCR after LCM. Am. J. Physiol. Cell Physiol. *284*, C220–C232.

Jones, R.C., and Murdoch, R.N. (1996). Regulation of the motility and metabolism of spermatozoa for storage in the epididymis of eutherian and marsupial mammals. Reprod. Fertil. Dev. *8*, 553–568.

Kondoh, G., Tojo, H., Nakatani, Y., Komazawa, N., Murata, C., Yamagata, K., Maeda, Y., Kinoshita, T., Okabe, M., Taguchi, R., and Takeda, J. (2005). Angiotensin-converting enzyme is a GPI-anchored protein releasing factor crucial for fertilization. Nat. Med. *11*, 160–166.

Krege, J.H., John, S.W., Langenbach, L.L., Hodgin, J.B., Hagaman, J.R., Bachman, E.S., Jennette, J.C., O'Brien, D.A., and Smithies, O. (1995). Male-female differences in fertility and blood pressure in ACE-deficient mice. Nature *375*, 146–148.

Lavker, R.M., Tseng, S.C., and Sun, T.T. (2004). Corneal epithelial stem cells at the limbus: looking at some old problems from a new angle. Exp. Eye Res. *78*, 433–446.

Leung, C.T., Coulombe, P.A., and Reed, R.R. (2007). Contribution of olfactory neural stem cells to tissue maintenance and regeneration. Nat. Neurosci. *10*, 720–726.

Leung, G.P., Cheung, K.H., Leung, C.T., Tsang, M.W., and Wong, P.Y. (2004). Regulation of epididymal principal cell functions by basal cells: role of transient receptor potential (Trp) proteins and cyclooxygenase-1 (COX-1). Mol. Cell. Endocrinol. *216*, 5–13.

Leung, P.S., Chan, H.C., Fu, L.X., Zhou, W.L., and Wong, P.Y. (1997). Angiotensin II receptors, AT1 and AT2 in the rat epididymis. Immunocytochemical and electrophysiological studies. Biochim. Biophys. Acta *1357*, 65–72.

Leung, P.S., and Sernia, C. (2003). The renin-angiotensin system and male reproduction: new functions for old hormones. J. Mol. Endocrinol. *30*, 263–270.

Mewe, M., Bauer, C.K., Muller, D., and Middendorff, R. (2006). Regulation of spontaneous contractile activity in the bovine epididymal duct by cyclic guanosine 5′-monophosphate-dependent pathways. Endocrinology *147*, 2051–2062.

Miller, R.L., Zhang, P., Smith, M., Beaulieu, V., Paunescu, T.G., Brown, D., Breton, S., and Nelson, R.D. (2005). V-ATPase B1-subunit promoter drives expression of EGFP in intercalated cells of kidney, clear cells of epididymis and airway cells of lung in transgenic mice. Am. J. Physiol. Cell Physiol. *288*, C1134–C1144.

Niess, J.H., Brand, S., Gu, X., Landsman, L., Jung, S., McCormick, B.A., Vyas, J.M., Boes, M., Ploegh, H.L., Fox, J.G., et al. (2005). CX3CR1-mediated dendritic cell access to the intestinal lumen and bacterial clearance. Science *307*, 254–258.

Parnot, C., and Kobilka, B. (2004). Toward understanding GPCR dimers. Nat. Struct. Mol. Biol. *11*, 691–692.

Pastor-Soler, N., Beaulieu, V., Litvin, T.N., Da Silva, N., Chen, Y., Brown, D., Buck, J., Levin, L.R., and Breton, S. (2003). Bicarbonate-regulated adenylyl cyclase (sAC) is a sensor that regulates pH-dependent V-ATPase recycling. J. Biol. Chem. *278*, 49523–49529.

Pastor-Soler, N., Hallows, K.R., Smolak, C., Gong, F., Brown, D., and Breton, S. (2008). Alkaline pH- and cAMP-induced V-ATPase membrane accumulation is mediated by protein kinase A in epididymal clear cells. Am. J. Physiol. Cell Physiol. *294*, C488–C494.

Pastor-Soler, N., Pietrement, C., and Breton, S. (2005). Role of acid/base transporters in the male reproductive tract and potential consequences of their malfunction. Physiology (Bethesda) *20*, 417–428.

Pech, V., Zheng, W., Pham, T.D., Verlander, J.W., and Wall, S.M. (2008). Angiotensin II activates H+-ATPase in type A intercalated cells. J. Am. Soc. Nephrol. *19*, 84–91.

Price, D. (1963). Comparative Aspects Of Development And Structure In The Prostate. Natl. Cancer Inst. Monogr. *12*, 1–27.

Rescigno, M., Urbano, M., Valzasina, B., Francolini, M., Rotta, G., Bonasio, R., Granucci, F., Kraehenbuhl, J.P., and Ricciardi-Castagnoli, P. (2001). Dendritic cells express tight junction proteins and penetrate gut epithelial monolayers to sample bacteria. Nat. Immunol. *2*, 361–367.

Rizzo, S., Attard, G., and Hudson, D.L. (2005). Prostate epithelial stem cells. Cell Prolif. *38*, 363–374.

Robaire, B., and Viger, R.S. (1995). Regulation of epididymal epithelial cell functions. Biol. Reprod. *52*, 226–236.

Rothenberger, F., Velic, A., Stehberger, P.A., Kovacikova, J., and Wagner, C.A. (2007). Angiotensin II stimulates vacuolar H+ -ATPase activity in renal acid-secretory intercalated cells from the outer medullary collecting duct. J. Am. Soc. Nephrol. *18*, 2085–2093.

Saez, F., Legare, C., Laflamme, J., and Sullivan, R. (2004). Vasectomy-dependent dysregulation of a local renin-angiotensin system in the epididymis of the cynomolgus monkey (Macaca fascicularis). J. Androl. *25*, 784–796.

Schneeberger, E.E., and Lynch, R.D. (2004). The tight junction: a multifunctional complex. Am. J. Physiol. Cell Physiol. *286*, C1213–C1228.

Skrabanek, L., Murcia, M., Bouvier, M., Devi, L., George, S.R., Lohse, M.J., Milligan, G., Neubig, R., Palczewski, K., Parmentier, M., et al. (2007). Requirements and ontology for a G protein-coupled receptor oligomerization knowledge base. BMC Bioinformatics *8*, 177.

Smith, P.J.S., Sanger, R.S., and Messerli, M.A. (2007). Principles, development and applications of self-referencing electrochemical microelectrodes to the determination of fluxes at cell membranes. In Methods and new frontiers in neuroscience, A.C. Michael, ed. (CRC Press), pp. 373–406.

Stein, B., Khew-Goodall, Y., Gamble, J., and Vadas, M.A. (1997). Transmigration of leukocytes. In Endothelium in Clinical Practice: Source and Target of NovelTherapies, G.M. Rubanyi and V.J. Dzau, eds. (New York: Marcel Dekker, Inc.), pp. 147–202.

Takano, K., Kojima, T., Go, M., Murata, M., Ichimiya, S., Himi, T., and Sawada, N. (2005). HLA-DR- and CD11c-positive dendritic cells penetrate beyond well-developed epithelial tight junctions in human nasal mucosa of allergic rhinitis. J. Histochem. Cytochem. *53*, 611–619.

Toda, N., Ayajiki, K., and Okamura, T. (2007). Interaction of endothelial nitric oxide and angiotensin in the circulation. Pharmacol. Rev. *59*, 54–87.

van Leenders, G.J., and Schalken, J.A. (2003). Epithelial cell differentiation in the human prostate epithelium: implications for the pathogenesis and therapy of prostate cancer. Crit. Rev. Oncol. Hematol. Suppl. *46*, S3–S10.

Veri, J.P., Hermo, L., and Robaire, B. (1993). Immunocytochemical localization of the Yf subunit of glutathione S-transferase P shows regional variation in the staining of epithelial cells of the testis, efferent ducts, and epididymis of the male rat. J. Androl. *14*, 23–44.

Wei, C., Willis, R.A., Tilton, B.R., Looney, R.J., Lord, E.M., Barth, R.K., and Frelinger, J.G. (1997). Tissue-specific expression of the human prostate-specific antigen gene in transgenic mice: implications for tolerance and immunotherapy. Proc. Natl. Acad. Sci. USA *94*, 6369–6374.

Wong, P.Y., and Yeung, C.H. (1978). Absorptive and secretory functions of the perfused rat cauda epididymidis. J. Physiol. *275*, 13–26.

Yeung, C.H., Nashan, D., Sorg, C., Oberpenning, F., Schulze, H., Nieschlag, E., and Cooper, T.G. (1994). Basal cells of the human epididymis–antigenic and ultrastructural similarities to tissue-fixed macrophages. Biol. Reprod. *50*, 917–926.

Zini, A., O'Bryan, M.K., Magid, M.S., and Schlegel, P.N. (1996). Immunohistochemical localization of endothelial nitric oxide synthase in human testis, epididymis, and vas deferens suggests a possible role for nitric oxide in spermatogenesis, sperm maturation, and programmed cell death. Biol. Reprod. *55*, 935–941.